

Input Robustification for Motion Control of Systems without Rigid-Body Mode

Yongkai Xu, Peter H. Meckl

Abstract—Robust proximate-time-optimal inputs can be obtained by carrying out the optimization scheme on an augmented system where the vibrational modes are purposely repeated. This method has been successfully implemented on systems with rigid-body mode in many researchers' work. However, the input robustification for systems without rigid-body mode poses a unique problem because of the time-unboundedness of the input. In this paper, a robustification scheme based on the command shaping technique of constrained least-square optimization is proposed to address this problem and an example is used to illustrate the process. To smooth out in-maneuver oscillation due to the fast maneuver, an energy optimization formulation is presented. The incorporation of the EI (extended insensitivity) technique is also explored to extend the robustness while maintaining a reasonable response speed.

I. INTRODUCTION

As pointed out in many publications, time-optimal input design is extremely sensitive to parameter perturbation and unmodeled dynamics. Therefore more robust proximate time-optimal controllers that give near time-optimal responses are desired [1].

N. C. Singer and W. P. Seering [2] proposed an input shaping method that uses a sequence impulses having appropriate amplitudes and switch times to achieve zero residual vibration at the end of travel. By adding extra impulses to the basic ZV (zero-vibration) shaper, some robustness to disturbances and model uncertainties is achieved.

P. H. Meckl et al. [3][4] constructed command profiles using a series of ramped sinusoids from which the harmonics that have significant spectral energy at the natural frequencies of the system have been discarded. By making the frequency troughs even wider, the command is made robust to frequency uncertainty of the system.

T. Singh and S. R. Vadali [5][6] formulated a parameter optimization problem to minimize the maneuver time with the constraint that the time-delay filter cancels all of the

Manuscript received September 27, 2004.

Yongkai Xu is with the School of Mechanical Engineering, Purdue University, West Lafayette, IN 47907 USA (phone: 765-494-2266; fax: 765-494-0539; e-mail: xuy@ purdue.edu).

Peter H. Meckl is with the School of Mechanical Engineering, Purdue University, West Lafayette, IN 47907 USA.

system poles, and addressed the robustness to modeling errors by placing multiple zeros of the filter at the estimated location of the system poles.

L. Y. Pao and W. E. Singhouse [7] investigated several time-optimal shapers, and showed that the robust time-optimal shaper design is equivalent to the traditional time-optimal control problem on an augmented system where the vibrational modes of the original model are purposely repeated. By locating multiple zeros at (or near) the system poles, the input is made less sensitive to model uncertainties (Fig. 1). This can be equivalently done by carrying out the time-optimal input design on an augmented

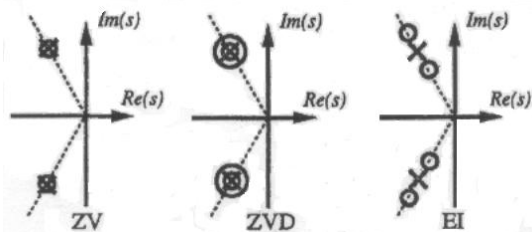


Fig. 1. Pole-zero maps in the s-plane illustrating how ZV, ZVD, and EI shapers place zeros at or near system poles (from [7])

system [8][9].

Input robustness from the zero-placing technique has been mathematically proved by S. P. Bhat and D. K. Miu [10] from the perspective of frequency domain. Assume an n -dimensional single-input system has been put into the Jordan canonical form as

$$\dot{\mathbf{q}}(t) = \mathbf{J}\mathbf{q}(t) + \mathbf{B}^*u(t) = \begin{bmatrix} \mathbf{J}_1 & & \\ & \ddots & \\ & & \mathbf{J}_n \end{bmatrix} \mathbf{q}(t) + \begin{bmatrix} \mathbf{B}_1^* \\ \vdots \\ \mathbf{B}_n^* \end{bmatrix} u(t) \quad (1)$$

where

$$\mathbf{J}_i = \begin{pmatrix} p_i & 1 & & \\ & p_i & & \\ & & \ddots & 1 \\ & & & p_i \end{pmatrix}, \mathbf{B}_i^* = \begin{pmatrix} 0 \\ 0 \\ \vdots \\ 1 \end{pmatrix}, \quad (i=1,\dots,n)$$

correspond to a pole p_i with multiplicity m_i . Thus the original system (1) can be decoupled into n sets of equations, each with a dimension m_i . The sufficient condition for input robustness is given as

$$\frac{1}{(m_i - j)!} \frac{d^{m_i-j}}{ds^{m_i-j}} U(s) \Big|_{s=p_i} = \sum_{k=j}^{m_i} \left[q_{ik}(T) \frac{(-T)^{k-j}}{(k-j)!} e^{-p_i T} \right] - q_{ij}(0) \quad (2)$$

For a system with rigid-body mode, zero residual vibration requires the final states of any vibrational modes to be identically zero, that is, $\mathbf{q}_i(T) = 0, i > 1$. With zero initial condition, (2) reduces to

$$\frac{d^m}{ds^m} U(s) \Big|_{s=p_i} = 0, \quad m = 0, 1, 2, \dots, m_i - 1 \quad (3)$$

For a system without rigid-body mode, however, $\mathbf{q}_i(T) \neq 0$ because of the set-point requirement. Then (2) results in $\left[d^m U(s)/ds^m \right]_{s=p_i} \neq 0$ for some m .

This may seem contradictory to the philosophy of zero residual vibration command shaping. However, Bhat and Miu's derivation is based on the assumption that $u(t)$ is time-bounded (Fig. 2(a)). This is the nature of the input for systems with rigid-body mode since the force can be removed once the system gets to the set-point. But this is not true for a system without rigid-body mode because a certain input has to be maintained in order to keep the system at the set-point (Fig. 2(b)).

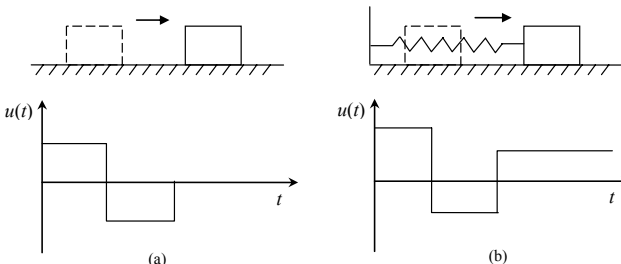


Fig. 2. Time-boundedness of input signals

Therefore, an input robustification method for systems without rigid-body mode is proposed in this paper. Before that we briefly introduce in Part II the time-optimal command shaping technique of constrained least-square optimization proposed by M. C. Reynolds and P. H. Meckl [11] since this is the platform of our proposed input robustification. The EI (extended-insensitivity) technique is also studied through an example. Simulation results of both point-to-point motion and trajectory tracking are presented as verification of the proposed method.

II. TIME-OPTIMAL COMMAND SHAPING

Given a discrete-time system

$$\begin{aligned} \mathbf{x}(k+1) &= \mathbf{A}\mathbf{x}(k) + \mathbf{B}u(k) \\ y(k) &= \mathbf{C}\mathbf{x}(k) \end{aligned} \quad (4)$$

and a tracking tolerance

$$|y(k) - y_d(k)| \leq e_{\text{allow}}(k) \quad (5)$$

the system output is

$$y(k) = \mathbf{C}\mathbf{A}^k \mathbf{x}(0) + \mathbf{C}\Phi \mathbf{U}(k) \quad (6)$$

where $\Phi = [\mathbf{A}^{k-1}\mathbf{B} \quad \mathbf{A}^{k-2}\mathbf{B} \quad \dots \quad \mathbf{B}]$, and

$$\mathbf{U}(k) = [u(0) \quad u(1) \quad \dots \quad u(k-1)]^T \quad (7)$$

It can be shown that the tracking constraint for the k -th sampling instant can be set up as

$$\begin{bmatrix} \mathbf{R} \\ -\mathbf{R} \end{bmatrix} \mathbf{U}(k) \leq \begin{bmatrix} f_1 \\ f_2 \end{bmatrix} \quad (8)$$

where $\mathbf{R} = \mathbf{C}\Phi$, and

$$\begin{aligned} f_1 &= y_d(k) + e_{\text{allow}}(k) - \mathbf{C}\mathbf{A}^k \mathbf{x}(0), \\ f_2 &= -y_d(k) + e_{\text{allow}}(k) + \mathbf{C}\mathbf{A}^k \mathbf{x}(0). \end{aligned}$$

Also the actuator has a saturation limit:

$$|u(k)| \leq F_{\max} \quad (9)$$

By incorporating the tracking constraint and actuator limit at each point on the trajectory in a least-square programming scheme, a time-optimal input profile can be obtained by increasing k until a solution satisfying the constraints results. The optimization problem is formulated as

$$\begin{aligned} \min_{\mathbf{U}(k)} \quad & \left\{ (\mathbf{x}(k) - \mathbf{x}_d)^T (\mathbf{x}(k) - \mathbf{x}_d) \right\}^{\frac{1}{2}}, \\ \text{subject to } & (8), (9) \end{aligned} \quad (10)$$

Many standard packages are available for solving linear least-square programming problems, including MATLAB.

III. ROBUSTIFICATION OF TIME-UNBOUNDED INPUT

A. Robustification scheme

Assume that the system has been put into the Jordan canonical form as in (1). We also assume that the system has no rigid-body mode and its input and output are shown in Fig. 3. To facilitate the discussion, we denote the input history before time T as $u_T(t)$, namely,

$$u_T(t) = \begin{cases} u(t), & 0 \leq t \leq T \\ 0, & t > T \end{cases} \quad (11)$$

Then the Laplace transform of $u(t)$ is

$$U(s) = \int_0^T u_T(t) e^{-st} dt + \int_T^\infty u_{ss} e^{-st} dt = U_T(s) + \frac{u_{ss}}{s} e^{-sT} \quad (12)$$

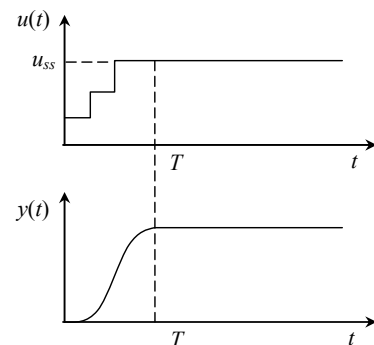


Fig. 3. Input and output of a system without rigid-body mode

Therefore,

$$U_T(s) = U(s) - \frac{u_{ss}}{s} e^{-sT} \quad (13)$$

Since $u_T(t)$ is a time-bounded signal, we can directly apply the sufficient condition (2), resulting in:

$$\frac{1}{(m_i - j)!} \frac{d^{m_i-j}}{ds^{m_i-j}} U_T(s) \Big|_{s=p_i} = \sum_{k=j}^{m_i} \left[q_{ik}(T) \frac{(-T)^{k-j}}{(k-j)!} e^{-p_i T} \right] - q_{ij}(0) \quad (14)$$

Substituting (13) into (14), the LHS becomes

$$\begin{aligned} & \frac{1}{(m_i - j)!} \frac{d^{m_i-j}}{ds^{m_i-j}} \left[U(s) - \frac{u_{ss}}{s} e^{-sT} \right] \Big|_{s=p_i} \\ &= \frac{1}{(m_i - j)!} \left\{ \frac{d^{m_i-j}}{ds^{m_i-j}} U(s) \Big|_{s=p_i} - \frac{d^{m_i-j}}{ds^{m_i-j}} \left[\frac{u_{ss}}{s} e^{-sT} \right] \Big|_{s=p_i} \right\} \end{aligned} \quad (15)$$

To simplify the notation, we denote

$$D_m(p_i) = \frac{d^m}{ds^m} \left[\frac{u_{ss}}{s} e^{-sT} \right] \Big|_{s=p_i} \quad (16)$$

Then (14) reduces to

$$\begin{aligned} & \frac{1}{(m_i - j)!} \frac{d^{m_i-j}}{ds^{m_i-j}} U(s) \Big|_{s=p_i} = \sum_{k=j}^{m_i} \left[q_{ik}(T) \frac{(-T)^{k-j}}{(k-j)!} e^{-p_i T} \right] \\ & \quad - q_{ij}(0) + \frac{1}{(m_i - j)!} D_{m_i-j}(p_i) \end{aligned} \quad (17)$$

Considering that in most system augmentations the multiplicity is usually $m_i \leq 3$, values for $(m_i - j)$ are shown in Table 1:

Table 1. Most common values of $(m_i - j)$

m_i	1	2		3	
j	1	1	2	1	2
$m_i - j$	0	1	0	2	1

The explicit expressions of $D_{m_i-j}(p_i)$ for m_i up to 3 are:

$$D_0(p_i) = \frac{u_{ss}}{p_i} e^{-p_i T} \quad (18.1)$$

$$D_1(p_i) = -\frac{u_{ss}}{p_i^2} e^{-p_i T} (1 + p_i T) \quad (18.2)$$

$$D_2(p_i) = \frac{u_{ss}}{p_i^3} e^{-p_i T} (2 + 2Tp_i + T^2 p_i^2) \quad (18.3)$$

In the rest of this paper, we call a robust input obtained using the augmented system with multiplicity $m+1$ for each mode as “ m -th order robust”.

B. Example

We illustrate the proposed input robustification method using an example of a single-mode system, whose transfer function is given by

$$G(s) = \frac{1}{s^2/\omega_0^2 + 1} \quad (19)$$

where $\omega_0 = 10$ rad/s. Put it into the Jordan canonical form

$$\begin{aligned} \begin{bmatrix} \dot{x}_1 \\ \dot{x}_2 \end{bmatrix} &= \begin{bmatrix} p & 0 \\ 0 & p^* \end{bmatrix} \begin{bmatrix} x_1 \\ x_2 \end{bmatrix} + \begin{bmatrix} 1 \\ 1 \end{bmatrix} u \\ y &= [c_1 \ c_2] \mathbf{x} \end{aligned} \quad (20)$$

where $p = j\omega_0$, $c_1 = -\frac{\omega_0}{2}j$, $c_2 = \frac{\omega_0}{2}j$. Assume the system is initially at rest. The steady-state values can be found as

$$\begin{bmatrix} x_{ss1} \\ x_{ss2} \end{bmatrix} = \begin{bmatrix} -\frac{u_{ss}}{p} & -\frac{u_{ss}}{p^*} \end{bmatrix}^T \quad (21)$$

Suppose a 2nd-order robust input is desired, we augment the system to $m_i = 3$ and the augmented system matrices are:

$$\begin{bmatrix} \dot{q}_{11} \\ \dot{q}_{12} \\ \dot{q}_{13} \\ \dot{q}_{21} \\ \dot{q}_{22} \\ \dot{q}_{23} \end{bmatrix} = \begin{bmatrix} p & 1 & | & & & \mathbf{0} \\ p & 1 & | & & & q_{11} \\ \hline p & | & p^* & | & 1 & q_{12} \\ \hline \mathbf{0} & | & p^* & | & 1 & q_{13} \\ \mathbf{0} & | & p^* & | & 1 & q_{21} \\ \mathbf{0} & | & p^* & | & 1 & q_{22} \\ \mathbf{0} & | & p^* & | & 1 & q_{23} \end{bmatrix} + \begin{bmatrix} 0 \\ 0 \\ 1 \\ 0 \\ 0 \\ 1 \end{bmatrix} u \quad (22)$$

$$y = [0 \ 0 \ c_1 \ 0 \ 0 \ c_2] \mathbf{q}$$

Let

$$q_{13} = x_{ss1} = -\frac{u_{ss}}{p}, \quad q_{23} = x_{ss2} = -\frac{u_{ss}}{p^*} \quad (23)$$

so that the set-point requirement is satisfied

$$y = c_1 q_{13} + c_2 q_{23} = [c_1 \ c_2] \mathbf{x}_{ss} = y_d \quad (24)$$

Here we only discuss for the pole p using (17) and (18). The case for the other pole p^* can be easily developed in the same manner.

$$(1) \ j = 3 \Rightarrow m_i - j = 0 :$$

$$\begin{aligned} U(s) \Big|_{s=p} &= q_{13}(T) e^{-pT} - q_{13}(0) + D_0(p) \\ &= -\frac{u_{ss}}{p} e^{-pT} - 0 + \frac{u_{ss}}{p} e^{-pT} \\ &= 0 \end{aligned} \quad (25)$$

$$(2) \ j = 2 \Rightarrow m_i - j = 1 :$$

$$\begin{aligned} \frac{d}{ds} U(s) \Big|_{s=p} &= [q_{12}(T) - Tq_{13}(T)] e^{-pT} - q_{12}(0) + D_1(p) \\ &= \left[q_{12}(T) + T \frac{u_{ss}}{p} \right] e^{-pT} - \frac{u_{ss}}{p^2} e^{-pT} (1 + pT) \\ &= \left[q_{12}(T) - \frac{u_{ss}}{p^2} \right] e^{-pT} \end{aligned} \quad (26)$$

Now that we have the freedom to choose $q_{12}(T)$ to make $\frac{d}{ds} U(s) \Big|_{s=p} = 0$, we set

$$q_{12}(T) = \frac{u_{ss}}{p^2} \quad (27)$$

$$(3) \ j = 1 \Rightarrow m_i - j = 2 :$$

$$\begin{aligned} \frac{d^2}{ds^2} U(s) |_{s=p} &= \left[q_{11}(T) - Tq_{12}(T) + \frac{T^2}{2!} q_{13}(T) \right] e^{-pT} \\ &\quad - q_{11}(0) + \frac{1}{2!} D_2(p) \\ &= \left[q_{11}(T) + \frac{u_{ss}}{p^3} \right] e^{-pT} \end{aligned} \quad (28)$$

By letting $\frac{d^2}{ds^2} U(s) |_{s=p} = 0$, we have

$$q_{11}(T) = -\frac{u_{ss}}{p^3} \quad (29)$$

Therefore, by choosing the final states of the augmented system as

$$\mathbf{q}_i(T) = \left[-\frac{u_{ss}}{p_i^3} \quad \frac{u_{ss}}{p_i^2} \quad -\frac{u_{ss}}{p_i} \right]^T \quad (30)$$

the optimization results in a 2nd-order robust input such that

$$U(s) |_{s=p_i} = \frac{d}{ds} U(s) |_{s=p_i} = \frac{d^2}{ds^2} U(s) |_{s=p_i} = 0 \quad (31)$$

It can be easily shown that, for a 1st-order robustification, by choosing the final states of the augmented system as

$$\mathbf{q}_i(T) = \left[\frac{u_{ss}}{p_i^2} \quad -\frac{u_{ss}}{p_i} \right]^T \quad (32)$$

the optimization results in a 1st-order robust input such that

$$U(s) |_{s=p_i} = \frac{d}{ds} U(s) |_{s=p_i} = 0 \quad (33)$$

The simulations of the non-robust and 1st-order robust inputs for the point-to-point maneuver (position from 0 to 1) of the example system are shown in Fig. 4 and Fig. 5, respectively. In both cases 10% perturbation to ω_0 was used to test the performance robustness. Obviously the output in Fig. 5 is more robust to the modeling error than the one in Fig. 4.

For comparison, we also designed a ZVD input shaper for the example system using the technique proposed by N.

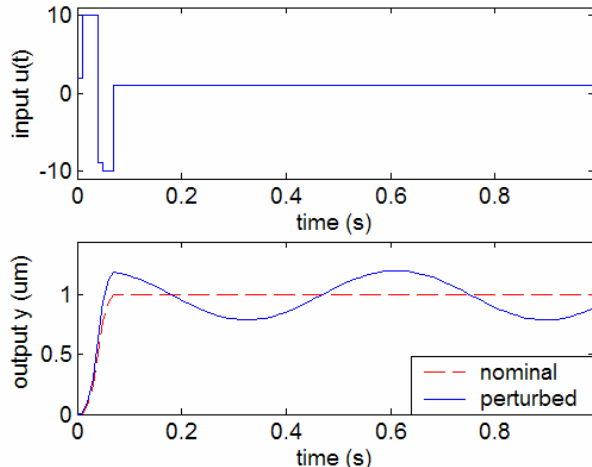


Fig. 4. Non-robust input and output

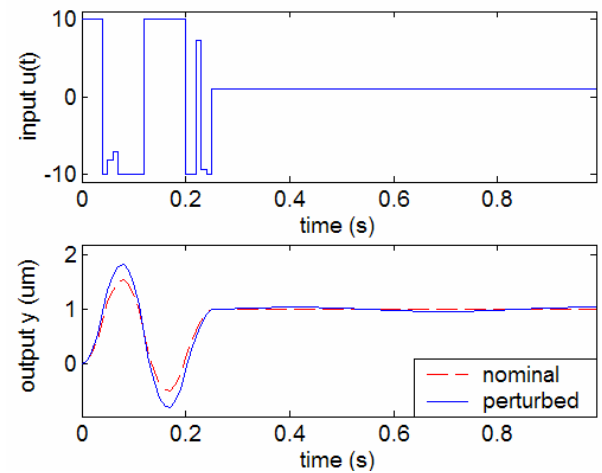


Fig. 5. 1st-order-robust input and output

C. Singer, and W. P. Seering [2]. The block diagram is shown in Fig. 6 and the simulation is shown in Fig. 7.

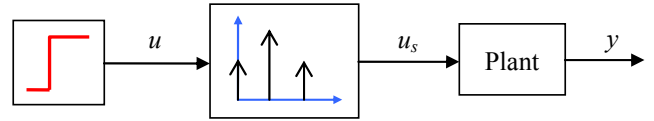


Fig. 6. Open loop system with ZVD shaper

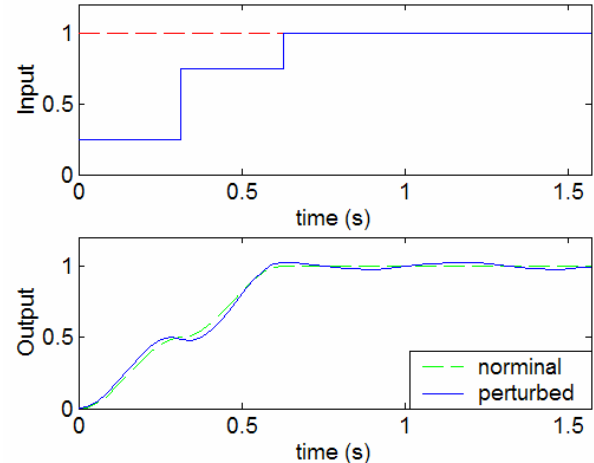


Fig. 7. ZVD shaped input and output

We observe that, with the same level of robustness, the maneuver time in Fig. 5 is less than half of that in Fig. 7, which means our proposed input robustification results in a much faster maneuver. The only price paid for the speed is a relatively larger in-maneuver oscillation. If this is a concern in a specific application, it can be addressed using the energy optimization scheme introduced in the next part.

C. Energy optimization scheme

The large in-maneuver oscillation occurs because the scheme seeks the time-optimal solution. The resulting input is such that the system is driven hard to move quickly, yet at the end of the motion the energy of the excited oscillation is released to achieve zero residual vibration.

For this reason, it can be expected that, if the time optimality requirement is relaxed and meanwhile the energy optimal solution is sought, the resulting robust input will be much smoother.

A new optimization problem is formulated as

$$J = \min_{\mathbf{U}} \frac{1}{2} \mathbf{U}^T \mathbf{U}$$

$$\text{subject to} \begin{cases} \text{(a) } \Phi \mathbf{U} = \mathbf{x}_d - \mathbf{A}^k \mathbf{x}_0 \\ \text{(b) actuator limit (9)} \\ \text{(c) tracking constraint (8) if applicable} \end{cases} \quad (34)$$

where constraint (a) is to satisfy the set-point requirement and achieve zero residual vibration. Fig. 8 shows a series of 1st-order robust inputs and outputs by relaxing the time optimality to different extent. In the figure, k is the number of steps of the maneuver. With the energy optimization scheme, we can trade off between the response speed and transition smoothness.

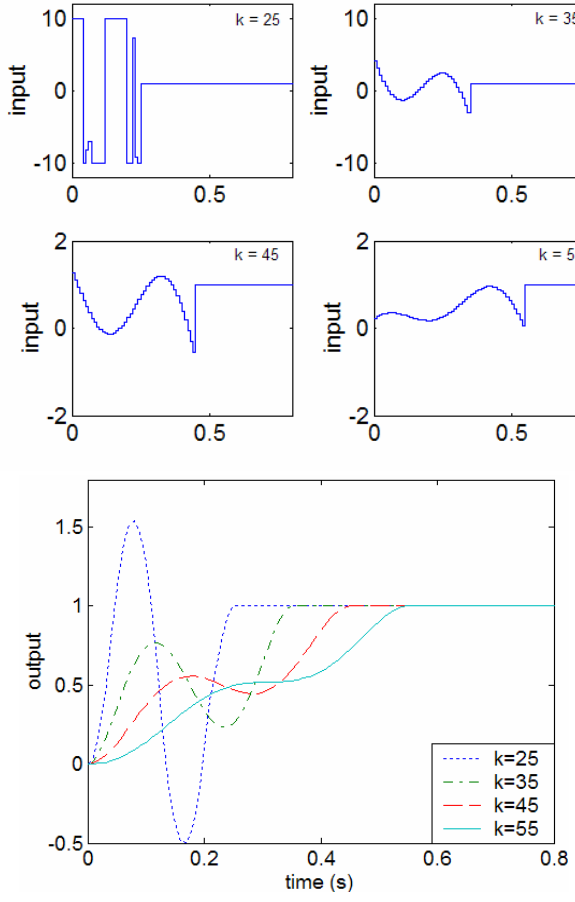


Fig. 8. 1st-order robust inputs and outputs from energy optimization

D. Trajectory tracking

Since the command shaping by least-square method has incorporated the tracking constraint, the proposed input robustification scheme can be directly applied to trajectory tracking cases without any change. Fig. 9 shows the

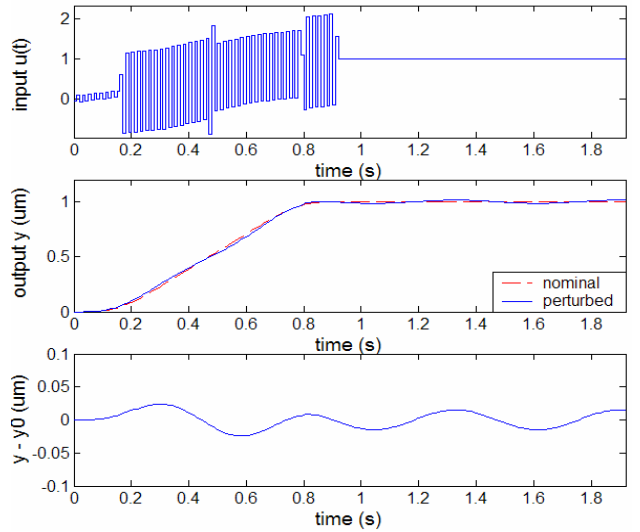


Fig. 9. 1st-order robust input and output with +10% perturbation

simulation result of the 1st-order robust input for tracking tolerance of 0.02. Again, 10% frequency perturbation was used to test the robustness.

It is a common understanding that the higher the order of the robustness, the longer the maneuver time. To speed up the response while maintaining a similar robustness, the EI (extended insensitivity) technique proposed by W. Singhouse et al. [12][13] can be used.

IV. EI ROBUSTIFICATION OF TIME-UNBOUNDED INPUT

As pointed out by Pao and Singhouse [7], EI inputs can be obtained by locating multiple zeros near (but not on) the system poles, which is equivalent to adding fictitious modes that are close to the original mode. This can also be easily incorporated into our proposed robustification scheme. Again, we use the plant in (19) as an example to illustrate the 1-hump EI robustification. The augmented system is

$$\begin{bmatrix} \dot{q}_{11} \\ \dot{q}_{12} \\ \dot{q}_{21} \\ \dot{q}_{22} \end{bmatrix} = \begin{bmatrix} j\omega_1 & & & \\ & -j\omega_1 & & \\ & & j\omega_2 & \\ & & & -j\omega_2 \end{bmatrix} \begin{bmatrix} q_{11} \\ q_{12} \\ q_{21} \\ q_{22} \end{bmatrix} + \begin{bmatrix} 1 \\ 1 \\ 1 \\ 1 \end{bmatrix} u \quad (35)$$

where $\omega_1 = \omega_0(1-\gamma)$, $\omega_2 = \omega_0(1+\gamma)$ and $\gamma > 0$ is the insensitivity range factor. The desired states at the end of the maneuver are chosen as

$$q_{11}(T) = -\frac{u_{ss}}{j\omega_i}, \quad q_{12}(T) = \frac{u_{ss}}{j\omega_i}, \quad i = 1, 2 \quad (36)$$

where the steady-state input value u_{ss} is determined in terms of the nominal frequency ω_0 to meet the set-point requirement. Fig. 10 compares the sensitivity curves of the 1-hump EI input (denoted as EI-1) and the 1st-order robust input (denoted as R-1) in Fig. 5 for point-to-point motion.

Note that the original mode doesn't show up in (35). Though this doesn't affect the robustification for point-to-

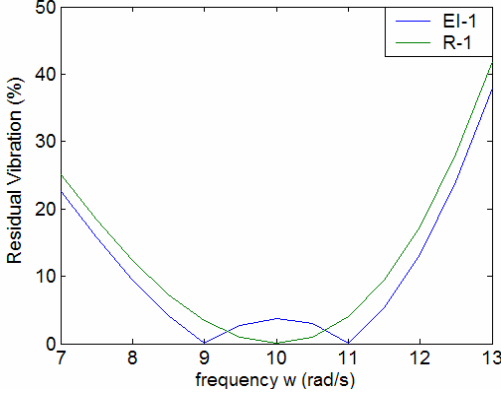


Fig. 10. Comparison of insensitivity curves

EI-1: 1-hump EI input; R-1: 1st-order robust inputs

point motion, it does influence trajectory tracking cases because the output of the augmented system is different from that of the original system. However, since the basic idea of the EI technique is to achieve an acceptably low level of vibration over a certain frequency range rather than zero vibration at the “nominal” frequency, the output of the augmented system doesn’t need to match the “nominal” exactly. Therefore, we can use either of the modes ω_1, ω_2 to form the tracking constraint. The output matrix can be augmented in either way:

$$C = \begin{bmatrix} -j\omega_1 & j\omega_1 & 0 & 0 \\ 0 & 0 & -j\omega_2 & j\omega_2 \end{bmatrix}, \quad C = \begin{bmatrix} 0 & 0 & -j\omega_2 & j\omega_2 \\ 0 & 0 & 0 & 0 \end{bmatrix} \quad (37)$$

The simulation results for the 1-hump EI tracking are shown in Fig 11. Compared with the 1st-order robust input for tracking in Fig. 9, its maneuver time is about the same, but it has more robustness than the 1st-order robust input.

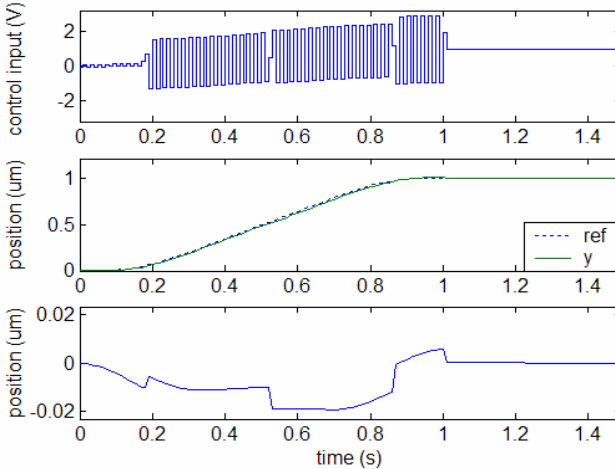


Fig. 11. 1-hump EI input and output of tracking control

V. CLOSED-LOOP IMPLEMENTATION

Although the time-optimal command is an open-loop signal, it can be easily incorporated into a closed-loop framework as illustrated in Fig. 12. The feedback controller is designed to provide additional robustness for unmodeled dynamics, disturbances, and computational delay in digital

implementation.

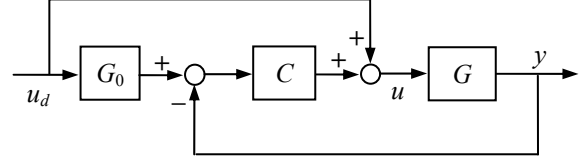


Fig. 12. Closed-loop implementation framework

VI. CONCLUSION

This paper introduced a robust command shaping technique to address the problem of systems without rigid-body mode caused by the time-unboundedness of the input. A new optimization that minimizes the input energy is formulated to reduce the in-maneuver oscillation. The EI technique is also incorporated to enhance the robustness while maintaining the same level of maneuver speed. Simulation results show the effectiveness of the proposed method.

REFERENCES

- [1] L. Y. Pao, and G. F. Franklin, “The robustness of a proximate time-optimal controller,” IEEE Transactions on Automatic Control, Vol. 39, No. 9, September 1994, pp. 1963-1966.
- [2] N. C. Singer, and W. P. Seering, “Preshaping command inputs to reduce system vibration,” Journal of Dynamic Systems, Measurement, and Control, Vol. 112, March 1990, pp. 76-82.
- [3] P. H. Meckl, and R. Kincer, “Robust motion control of flexible systems using feedforward forcing functions,” IEEE Transactions on Control Systems Technology, Vol. 2, No. 3, September 1994, pp. 245-254.
- [4] P. H. Meckl, and W. P. Seering, “Reducing residual vibration in systems with uncertain resonances,” IEEE Control Systems Magazine, April 1988, pp. 73-76.
- [5] T. Singh, and S. R. Vadali, “Robust time-optimal control: frequency domain approach,” Journal of Guidance, Control, and Dynamics, Vol. 17, No. 2, March-April 1994, pp. 346-353.
- [6] T. Singh, and S. R. Vadali, “Robust time-delay control,” Journal of Dynamic Systems, Measurement, and Control, Vol. 115, June 1993, pp. 303-306.
- [7] L. Y. Pao, and W. E. Singhouse, “On the equivalence of minimum time input shaping with traditional time-optimal control,” 1995 IEEE, pp. 1120-1125.
- [8] L. Y. Pao, “Minimum-time control characteristics of flexible structures,” Journal of Guidance, Control, and Dynamics, Vol. 19, No. 1, January-February 1996, pp. 123-129.
- [9] L. Y. Pao, “Verifying robust time-optimal commands for multimode flexible spacecraft,” Journal of Guidance, Vol. 20, No. 4, 1997, pp. 831-833.
- [10] S. P. Bhat, and D. K. Miu, “Precise point-to-point positioning control of flexible structures,” Journal of Dynamic Systems, Measurement, and Control, Vol. 112, December 1990, pp. 667-674.
- [11] M. C. Reynolds, and P. Meckl, “The application of command shaping to the tracking problem,” Proceedings of the American Control Conference, June 2003, pp. 3148-3153.
- [12] W. Singhouse, W. Seering, and N. Singer, “Residual vibration reduction using vector diagrams to generate shaped inputs,” Journal of Mechanical Design, Vol. 116, June 1994, pp. 654-659.
- [13] W. E. Singhouse, L. J. Porter, and N. C. Singer, “Vibration reduction using multi-hump extra-insensitive input shapers,” Proceedings of American Control Conference, June 1995, pp. 3830-3834.